Carbohydrate Polymers 87 (2012) 2447–2454

Contents lists available at SciVerse ScienceDirect

Carbohydrate Polymers

journal homepage: www.elsevier.com/locate/carbpol

Crystallization behavior and hydrophobic properties of biodegradable ethyl cellulose-g-poly(3-hydroxybutyrate-co-3-hydroxyvalerate): The influence of the side-chain length and grafting density

Hou-Yong Yu, Zong-Yi Qin*, Ling-Feng Wang, Zhe Zhou*

State Key Laboratory for Modification of Chemical Fibers and Polymer Materials, and College of Materials Science and Engineering, Donghua University, Shanghai 201620, China

ARTICLE INFO

Article history:
Received 1 February 2011
Received in revised form 2 November 2011
Accepted 7 November 2011
Available online 15 November 2011

Keywords:
Ethyl cellulose
Poly(3-hydroxybutyrate-co-3-hydroxyvalerate)
Graft copolymer
Crystallization behavior
Hydrophobic property

ABSTRACT

The copolymerization of grafting poly(3-hydroxybutyrate-co-3-hydroxyvalerate) (PHBV) onto ethyl cellulose (EC) was carried out through the homogeneous acylation reaction between EC as a backbone and telechelic OH-terminated PHBV oligomer as side chains in 1,2-dichloroethane by using 1,6-hexamethylene diisocyanate (HDI) as a coupling agent and dibutyltin dilaurate as catalyst. The resulting copolymers were studied by using NMR, FT-IR, WAXD, DSC, and contact angle measurements. It is found that with the increasing of the HDI/PHBV fraction, a transition exhibition occurred on crystallization behavior and hydrophobic properties, which could be modulated through controlling the lengths and grafting densities of PHBV side chains. Compared with those of neat PHBV, the degree of crystallinity for EC-g-PHBV$_{1.8}$ decreased from 58.1% to 39.1%, the maximum decomposition temperature increased from 259.6 to 266.3 °C, and the contact angle increased from 60.1° to 95.7°.

1. Introduction

Biodegradable polymer materials have attracted great scientific and technological interests due to their important applications, such as tissue engineering scaffolds, temporary prostheses, and controlled/sustained release drug delivery vehicles (Chen & Wu, 2005; Hu, Wei, Zhao, Liu, & Chen, 2009; Jack et al., 2009; Langer & Tirrell, 2004). Among biodegradable materials, bacterially synthesized poly(3-hydroxybutyrate-co-3-hydroxyvalerate) (PHBV) has been demonstrated as a potential biomedical material due to its good biocompatibility, nontoxicity, and compatibility with tissue and blood (Chen & Wu, 2005; Chen, Cheng, Li, Xu, & Chen, 2009; Hu, Jou, & Yang, 2004; Ke, Wang, Renb, Zhao, & Huang, 2010; Sultana & Wang, 2008). However, there are several shortcomings for the commercial use of the PHBV generally with less than 15 mol% fraction of hydroxyvalerate (3HV), such as brittleness caused by high crystallinity, thermal instability, and relatively narrow processing window (Ha & Cho, 2002; Liu, Zhu, Wu, & Qin, 2009; Yoshie, Saito, & Inoue, 2004). On the other hand, PHBV with high crystallinity has exhibited a remarkably long in vivo degradation time (Kose, Tezcaner, & Hasirci, 2002). It is further found that the amorphous regions typically biodegrade at a greater rate than the crystalline regions, and crystallinity can influence the biodegradability and cellular responses of the scaffolds. Generally, the crystallinity and hydrophobicity are the important factors to affect the biocompatibility and the platelet adhesion behavior on the surfaces of biodegradable materials (Chen, Cheng, & Xu, 2009; Chen & Wu, 2005; Hu et al., 2009; Jansen et al., 2005).

For the practical biomedical applications as biodegradable polymeric scaffolds, the controlled degradation rate and good biocompatibility are needed (Chen, Cheng, Xu, et al., 2009; Ha & Cho, 2002; Sultana & Wang, 2008). Much of these success has been achieved through judicious selection of existing materials with specific chemical modification for controlling chemical component and microstructure, further changing its crystallinity and hydrophobicity to obtain expected degradation properties and biocompatibility and so on (Chen, Cheng, Li, et al., 2009; Chen, Cheng, Xu, et al., 2009; Li et al., 2009; Sultana & Wang, 2008). It has been found that PHBV films with the reduced crystallinity could exhibit fairly regular and smooth surface, which were benefited to cell attachment and growth (Chen & Wu, 2005), while the lowered melting temperature (T_m) well below the thermal decomposition temperature makes PHBV easier to process. In addition, the rate of enzymatic degradation of PHBV increases with a decrease in the degree of crystallinity (Ha & Cho, 2002; Sato et al., 2004; Sultana & Wang, 2008).

Blending PHBV with other biodegradable polymers is a practical and economical approach to tailor its crystallization behavior,

* Corresponding authors. Tel.: +86 21 67792861; fax: +86 21 67792855.
E-mail addresses: phqin@dhu.edu.cn (Z.-Y. Qin), zzhe@dhu.edu.cn (Z. Zhou).

0144-8617/$ – see front matter © 2011 Elsevier Ltd. All rights reserved.
doi:10.1016/j.carbpol.2011.11.022

degradation rate and other material properties, which has several technical advantages in comparison to the syntheses of new copolyesters, such as easy processing ability, balanced properties and low production costs (Ha & Cho, 2002; Yoshie et al., 2004; Yu, Dean, & Li, 2006). It has been reported that "green" composites were successfully fabricated by blending biodegradable polyester with cellulosic materials, such as ethyl cellulose (EC) (Finelli, Scandola, & Sadocco, 1998; Suthar, Pratap, & Raval, 2000; Zhang, Deng, & Huang, 1997), cellulose esters (Ceccorulli, Pizzoli, & Scandola, 1993; Yu et al., 2006), and recycled cellulose fibers (Bhardwaj, Mohanty, Drzal, Pourboghrat, & Misra, 2006).

Ethyl cellulose (EC) as a kind of chemically modified cellulose exhibits excellent plasticity, good solubility in organic solvents, biocompatibility, high mechanical intensity, good heat-resistance, cold-resistance and stability (Aggour & Abdel-Razik, 1999; Yuan, Yuan, Zhang, & Xie, 2007; Zhu, Dong, Wang, & Wang, 2010). It can be expected that the existence of the hydrogen bonding between the residual hydroxyl groups from the ethyl cellulose and carbonyl groups in PHBV would enhance thermal decomposition temperature and improve greatly the interfacial adhesion in the composites (Suthar et al., 2000; Zhang et al., 1997). Although two components were not miscible, the composites showed good 'mechanical compatibility'. More fortunately, the copolymers with ethyl cellulose as a hydrophobic backbone exhibit a number of very interesting properties such as biocompatibility and biodegradability (Lao, Renard, Linossier, Langlois, & Vallée-Rehel, 2007; Yan et al., 2009; Yuan et al., 2007). For instance, the melting temperatures of the copolymers through grafting poly(p-dioxanone) (PPDO) onto EC backbone can be increased, whereas the degradability of graft copolymers was decreased with the increasing of the side-chain length of crystalline PPDO (Zhu et al., 2010). For ethyl cellulose-graft-poly(ε-caprolactone) copolymer, controllable stepwise biodegradation properties and the improved thermal properties can be observed by adjusting the molar ratios of CL monomer to EC (Yuan et al., 2007). Recently, cellulose-based dual graft molecular brushes composed of ethyl cellulose-graft-poly(N,N-dimethylaminoethyl methacrylate)-graft-poly(ε-caprolactone) (EC-g-PDMAEMA-g-PCL) were prepared, which exhibited some unique physicochemical properties and multifunction due to their unique graft structures (Yan et al., 2009). Obviously, grafting biodegradable polymers onto EC backbone will open up entire research fields in biomedical biomaterials. More importantly, lowering the crystallinity and augmenting the hydrophobicity of cellulose-based materials are well-known approaches to improve their biodegradability in vitro. In this work, novel biodegradable graft copolymers combining the advantages of EC backbone and PHBV side chains were prepared, and an efficient modulation approach for the crystallinity and hydrophobicity of the copolymer would be presented by introducing different lengths and grafting densities of PHBV side chains.

2. Experimental

2.1. Materials

Poly(3-hydroxybutyrate-co-3-hydroxyvalerate) (PHBV) ($M_n = 5.90 \times 10^4$, $M_w = 1.58 \times 10^5$, and the molar ratio of HV is 2.57%) was purchased from Tiannan Biological Material Co., Ltd. (Ningbo, China). Ethyl cellulose (EC) ($M_n = 4.58 \times 10^4$, $M_w = 1.78 \times 10^5$, and the degree of ethyl substitution was 2.1) was obtained from Shanghai Chemical Reagent Co., Ltd. and dried at 70 °C for 48 h under vacuum before use. Ethanol (99.8%), diglyme, chloroform, ethylene glycol, dibutyltin dilaurate (90.0%), 1,2-dichloroethane (99.0%), and $CaCl_2$ were purchased from the Shanghai Guoyao Group Chemical Reagent Co., Ltd. (Shanghai, China). 1,6-Hexamethylene diisocyanate (HDI) (99.0%) was purchased from Aldrich (USA). 1,2-Dichloroethane was distilled over $CaCl_2$ before use and other reagents were used as received without further purification.

2.2. Synthesis of EC-g-PHBV copolymers

Telechelic OH-terminated PHBV oligomers with well-defined, predominantly reactive end groups were prepared by a transesterification procedure as described previously (Chen, Cheng, Xu, et al., 2009; Hirt, Neuenschwander, & Suter, 1996), and the reaction was illustrated as shown in Scheme 1. The detailed synthesis process was as follows: Commercial PHBV powder was dissolved in hot chloroform, reprecipitated with methanol to further purify the product, and dried in the vacuum oven at 60 °C. Then 30 g purified PHBV and 300 mL of diglyme were placed in a 500 mL four-necked round bottom flask with a mechanical stirrer, nitrogen inlet and outlet. A continuous nitrogen stream was kept under the surface of the liquid. Then the flask was heated to 140 °C in an oil bath with continuously mechanical stirring. After PHBV was dissolved completely, 60 mL of ethylene glycol and 0.3 g dibutyltin dilaurate as catalyst were quickly added to the flask. After a desired reaction time of 7.5 h, the products were precipitated with ethanol, washed repeatedly with ethanol, and dried under vacuum.

EC-g-PHBV copolymers were synthesized by using HDI as a coupling reagent via the synthetic pathway as shown in Scheme 1. The grafting conditions, such as the reaction time, temperature and mass ratio of PHBV oligomer to EC, were optimized to obtain the maximum grafting percentage. The PHBV/EC mass ratio can be optimized according to the number of functional groups, but it did not mean that all the PHBV could be successfully grafted onto the EC backbone. It is found that the larger grafting percentage can be achieved for the PHBV/EC ratio of 4:1 (120%) with the HDI/PHBV fraction of 1.8 than those for the PHBV/EC ratio of 6:1 (118%) and 2:1 (117%) under similar reaction conditions. Hence, the PHBV/EC mass ratio was chosen to be 4:1 in this work, and the effects of the HDI/PHBV fraction on structures of the EC-g-PHBV copolymers were further studied. The detailed synthesis process was as follows: 4.0 g PHBV oligomer, 1.0 g EC and 80 mL of anhydrous 1,2-dichloroethane were added into a 250 mL four-neck flask with a mechanical stirrer, nitrogen inlet and outlet. Then the flask was heated to 90 °C in an oil bath with mechanical stirring. After any trace water of the stirred mixture was removed through azeotropic distillation, only 20 mL of 1,2-dichloroethane remained in the flask. When the flask was cooled to 75 °C, various HDI fractions and ten drops of dibutyltin dilaurate were sequentially added into the flask. The reaction mixture was stirred at 75 °C for 48 h under a constant flow of nitrogen. After cooling to room temperature, the as-prepared products were redissolved into chloroform to remove the crosslinked substances, and followed by precipitation in a mixture of anhydrous alcohol and petroleum ether twice to remove the unreacted substances. The purified products were finally dried under vacuum at 40 °C for 24 h. The resulting copolymers were designated as EC-g-PHBV$_x$, where x denoted the HDI/PHBV fraction (molar ratio). The tested films for static contact angle test were prepared by dissolving the copolymer in chloroform (10 wt.%) and cast into thin sheets.

The grafting yield was recorded to calculate the grafting percentage (GP%) as a ratio of the increase of mass of EC divided by the starting mass of EC according to the following equation: grafting percentage (GP%) = $100 \times (m_C - m_{EC})/m_{EC}$, where m_C, m_{EC} and m_{PH} were the weights of extract graft product, ethyl cellulose, and PHBV, respectively. The grafting efficiency (GE%) and weight conversion (WC%) were also calculated by the following equation: grafting efficiency (GE%) = $100 \times (m_C - m_{EC})/m_{PH}$ and weight conversion (WC%) = $100 \times m_C/m_{PH}$, respectively.

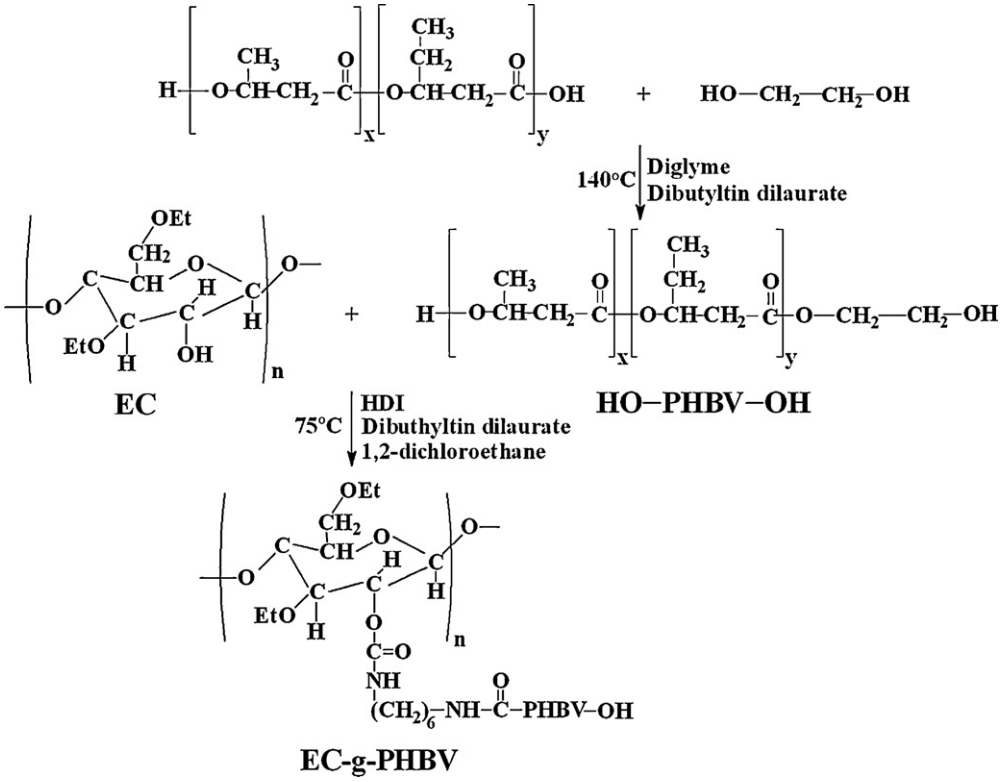

Scheme 1. Synthesis of EC-g-PHBV copolymer.

In addition, the number average molecular weight ($M_{n,th}$) could be calculated according to the following equation: $M_{n,th} = (M_{glucose} + M_{PHBV} \times [(m_C - m_{EC})/1980]/(m_{EC}/224)) \times n_{glucose}$, where 1980 g mol^{-1} is the molecular weight of telechelic OH-terminated PHBV oligomers (M_{PHBV}); 224 g mol^{-1} is the molecular weight of glucose unit of the EC backbone ($M_{glucose}$); $n_{glucose}$ is the numbers of glucose units of the EC backbone.

2.3. Characterization

The ^{13}C NMR and ^{1}H NMR spectra of PHBV, EC and the resulting copolymers were obtained from a Bruker Avance 400 NMR spectrometer in 5 mm tubes with $CDCl_3$ as a solvent at room temperature. FT-IR spectra were recorded on a Nicolet Nexus 670 FT-IR spectrophotometer; 32 scans were signal-averaged with a resolution of 4 cm^{-1} at room temperature. Wide-angle XRD measurements were carried out on a RIGAKU D/Max-2550 PC diffractometer with an area detector operating under Cu Kα (1.5418 Å) radiation (40 kV, 40 mA) at room temperature.

DSC measurements of PHBV, EC and the resulting copolymers were performed on MDSC TA-2910 differential scanning calorimeter by employing a 40 mL min^{-1}, flow of dry nitrogen as a purge gas for the sample and reference cells. The samples were firstly heated from room temperature to 200 °C at a heating rate of 20 °C min^{-1} (the first heating process), and maintained at this temperature for 5 min to remove the thermal history. Subsequently, the samples were cooled to 0 °C at 10 °C min^{-1} (the first cooling traces). Then the samples were again heated from 0 to 200 °C at 10 °C min^{-1} (the second heating traces). The non-isothermal crystallization behavior and melting behavior were analyzed based on the cooling traces and the second heating traces. TGA was carried out using Netzsch TG209 F1 TGA instrument coupled with QMS. The samples were heated at 10 °C min^{-1} from room temperature to 500 °C in a dynamic nitrogen atmosphere with the flow rate of 30 mL min^{-1}.

The contact angles of the PHBV, EC and the resulting copolymer were measured on the air surface of their films using pendant drop method on a Dataphysics OCA40 contact angle analyzer at room temperature. About 2 μL of deionized water was dropped onto the surface at a contact time of 5 s. Twenty independent determinations at different sites of the sample were averaged.

3. Results and discussion

3.1. Chemical structure: ^{13}C and ^{1}H NMR spectra

NMR spectra were used to verify the formation of the graft copolymers as shown in Fig. 1. All the characteristic peaks of PHBV and EC appeared in the spectra of the copolymers. As an example, Fig. 1(a) gave the ^{13}C NMR spectra of EC-g-PHBV$_{1.6}$ copolymer. The single characteristic peak of PHBV (labeled as peak 4 and 9) located at δ = 171.45 ppm was attributed to carbonyl group (–C=O) in the 3-hydroxybutyrate (HB) and 3-hydroxyvalerate (HV) units. A single peak (peak 10) at δ = 63.14 ppm and the multiple peaks (peak 11) at δ = 66.42–68.40 ppm were attributed to methylene group (–CH_2–OH), which formed during the transesterification reaction for preparing telechelic OH-terminated PHBV (Chen, Cheng, Xu, et al., 2009). The multiple peaks (peak a) at δ = 67.01–71.02 ppm were assigned to the methylene group (–CH_2–O–) in the glucose of EC, and a single peak (peak b) at δ = 17.03 ppm attributed to methyl group (–CH_3) (Lao et al., 2007; Yan et al., 2009; Yuan et al., 2007). A new peak (peak 12) at δ = 32.27 ppm belonged to the methylene group (–CH_2–NH–) from HDI demonstrated that the graft copolymerization was successfully achieved. The acylation reaction should mainly occur at C–2–OH or C–3–OH position, when EC with the degree of ethyl substitution of 2.1 was employed (Kang et al., 2006). Meanwhile, ^{1}H NMR gave clearly the nature of the proton species of EC-g-PHBV as shown in Fig. 1(b). The peaks around 5.21–5.33 ppm, and strong peaks at 2.52 and 2.30 ppm were

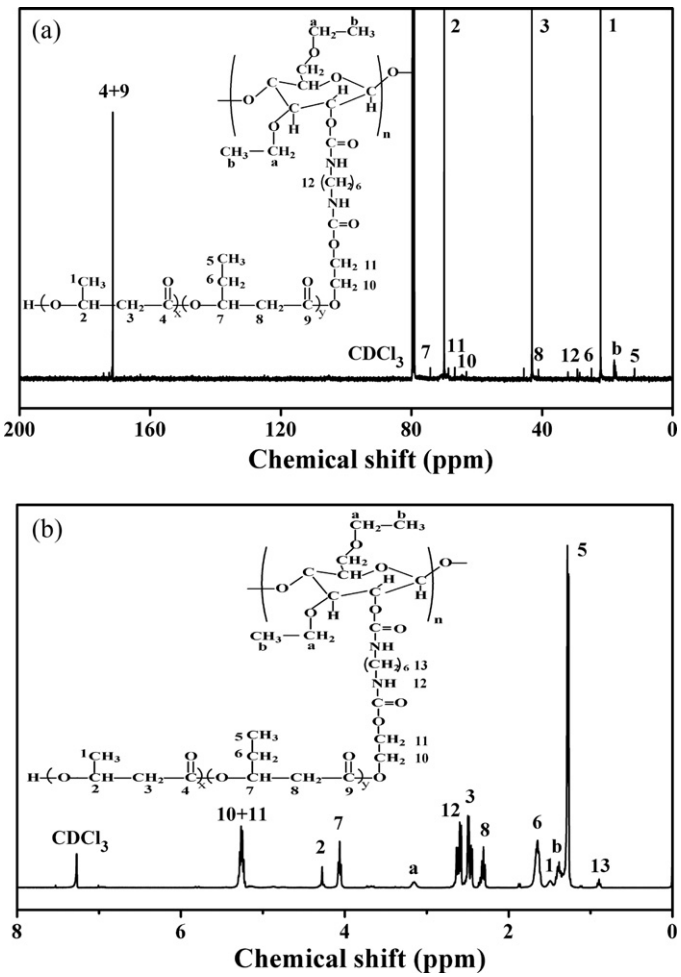

Fig. 1. ^{13}C NMR (a) and ^{1}H NMR (b) spectra of EC-g-PHBV$_{1.6}$ copolymer.

attributed to the terminal methylene protons (H_{10}, H_{11}) and the internal methylene protons (H_3, H_8) of PHBV side chain, respectively. The peaks at 1.36 ppm and around 3.11–3.35 ppm were assigned to the $-CH_3$ proton (H_b) of ethoxy group and the protons (H_a) including the glucose unit and the $-CH_2$ of ethoxy group of EC backbone (Yan et al., 2009; Zhu et al., 2010). New multiple peaks around 2.55–2.66 ppm were belonged to the –NH–COO proton of HDI, which also indicated that the graft copolymers were successfully prepared. Moreover, the lengths and the grafting density of graft side chains can be characterized by the degree of polymerization of PHBV (DP) and the degree of substitution of copolymer (DS), respectively (Zhu et al., 2010). DP, DS and the number average molecular weight of the copolymer ($M_{n,NMR}$) can be obtained through peak intensity calculations from ^{1}H NMR spectra, respectively.

$$\mathrm{DP} = \left(\frac{I_3 + I_{10}}{I_{10}}\right) \quad (1)$$

$$\mathrm{DS} = \left(\frac{2.1 \times 3 \times I_5}{2 \times I_b}\right) \quad (2)$$

$$M_{n,NMR} = 45,800 + \mathrm{DS} \times \mathrm{DP} \times 1980 \quad (3)$$

where I_3, I_5, I_{10} and I_b are the integral peak areas of methylene group, methyl group and methylene group of PHBV oligomers, and methyl group of EC, respectively. Further, 2.1 is the ethoxy substitution of EC, 1980 g mol^{-1} is the molecular weight of telechelic OH-terminated PHBV oligomers, and 45,800 g mol^{-1} is the molecular weight of EC.

Table 1 summarized the grafting parameters (GP%, GE% and WC%), the structure parameters (DS and DP), and the molecular weight ($M_{n,th}$ and $M_{n,NMR}$) for the copolymers prepared at the different HDI/PHBV fraction. When the fraction changed from 1.2 to 1.8, the values of GP%, GE% and WC% almost progressively increased from 85%, 21.25% and 46.25% to 120%, 30.0% and 55.0%, respectively. However, for the HDI/PHBV fraction of 2.1, these values decreased to 118%, 29.5% and 54.5%, respectively. Similar changes in trend for $M_{n,th}$, $M_{n,NMR}$ and DS can be found, whereas the DP increased gradually with the HDI/PHBV fraction. These results indicated that the hydroxyl groups of the EC backbone could effectively initiated graft polymerization with PHBV segments via the HDI coupling agent. On the one hand, the isocyanate groups of HDI would link hydroxyl groups of EC to hydroxyl groups of PHBV, which determine the grafting density. On the other hand, HDI was also active in connecting PHBV oligomers, which determine the length of side chain. When the graft side chains was long enough, the end hydroxyl group could not initiate graft polymerization due to the strong excluded volume effects of long chains, and thus only relatively short side chains would be grafted into EC backbone. It implied that the side-chain length and grafting density of the copolymer could be adjusted through changing the HDI/PHBV fractions. With the increasing of the HDI/PHBV fraction, the grafting structure of the copolymer changed from relatively long side chain with low grafting density, to board length distribution and relative high grafting density, and then more long side chain with high grafting density.

3.2. Chemical structure: FT-IR spectra

Fig. 2(a) shows the FT-IR spectra of EC, PHBV and the resulting copolymers. All the characteristic peaks of PHBV and EC appeared in the FT-IR spectra of the copolymers. For example, the bands at 1055 and 2867 cm^{-1} were assigned to –C–O–C– stretching vibration and CH_2 asymmetric stretching modes of EC, respectively. The bands at 1182, 1261, 1283, 1379, 1456, 1723, 2929 and 2979 cm^{-1} were attributed to stretching vibration of –C–O–C–, bending modes of the C–H, stretching vibration of C=O in ester, and symmetric and asymmetric stretching vibration of CH_3 of PHBV, respectively (Liu et al., 2009; Suthar et al., 2000). Compared with that of neat EC and PHBV, the intensity of O–H stretching for the glucose rings of EC around 3481 cm^{-1} decreased obviously, and the O–H stretching band of PHBV segment at 3436 cm^{-1} even disappeared in the spectra of the copolymers. This implied the terminal hydroxyl groups of PHBV were consumed in reaction with hydroxyl groups of EC through HDI as the coupling agent. More importantly, two new bands appeared at 1527 and 3391 cm^{-1} can be contributed to the medium bending vibration and symmetric stretching vibration of N–H from imino group (–OOCNH–) of polyurethane linkage, respectively (Chen, Cheng, Li, et al., 2009). Furthermore, an increase in the intensity of some characteristic bands for PHBV occurred with the increasing of the HDI/PHBV fraction as shown in Fig. 2(b), such as the increase in the bands at 2929 and 2979 cm^{-1} belonging to the CH_3 stretching vibration from side pendant alkyl groups of PHBV. This indicated an increasing content of PHBV in copolymers with the increasing of the HDI/PHBV fraction.

To better evaluate the graft length of PHBV side chains on crystallization of EC-g-PHBV copolymers, the area ratio of the bands situated at 1740 and 1723 cm^{-1} (A_{1740}/A_{1723}) was calculated and listed in Table 2. It has been reported that the carbonyl stretching vibration band at 1723 cm^{-1} and its shoulder at 1740 cm^{-1} were related to the crystalline and amorphous components in PHBV, respectively (Lao et al., 2007; Zhang et al., 1997). Table 2 shows that with the increase of the HDI/PHBV fraction, the A_{1740}/A_{1723} values decreased greatly from 1.16 for EC-g-PHBV$_{1.2}$ to 0.71 for EC-g-PHBV$_{1.8}$, finally increased to 0.74 for EC-g-PHBV$_{2.1}$. It is well known that the mobility of long side chains for linear polymer is easier

Table 1
The grafting parameters, the structure parameters and the number average molecular weight for EC-g-PHBV copolymers prepared under various HDI/PHBV fractions.

Sample	GP%	GE%	WC%	$M_{n,th}$ (g mol^{-1})[a]	DP[b]	DS[b]	$M_{n,NMR}$ (g mol^{-1})[b]
EC-g-PHBV$_{1.2}$	85	21.25	46.25	82,048.8	25.2	0.30	60,768.8
EC-g-PHBV$_{1.5}$	93	23.25	48.25	90,127.2	28.5	0.34	64,986.2
EC-g-PHBV$_{1.6}$	107	26.75	51.75	94,166.4	33.1	0.45	75,292.1
EC-g-PHBV$_{1.8}$	120	30.0	55.0	100,629.1	40.6	0.56	90,817.3
EC-g-PHBV$_{2.1}$	118	29.5	54.5	99,821.3	42.3	0.53	90,189.6

[a] $M_{n,th}$ is determined by mass of the products.
[b] $M_{n,NMR}$ is determined by ^{1}H NMR spectroscopy.

Table 2
The A_{1740}/A_{1723} value, the degree of crystallinity and the thermal parameters for PHBV, EC and the resulting copolymers under various HDI/PHBV fractions.

Sample	A_{1740}/A_{1723}[a]	X_c (%)[b]	T_{cc} (°C)	ΔH_{cc} (J g^{-1})	ΔH_{m2} (J g^{-1})	T_{m1} (°C)	T_{m2} (°C)	T_{max} (°C)
PHBV	2.25	58.1	–	–	49.2	135.9	150.9	259.6
EC	–	–	–	–	1.7	177.5	–	364.4
EC-g-PHBV$_{1.2}$	1.16	43.6	86.8	4.3	10.1	122.0	134.8	272.6
EC-g-PHBV$_{1.5}$	1.07	41.5	85.7	5.8	8.5	123.1	135.9	267.7
EC-g-PHBV$_{1.6}$	0.79	40.2	80.5	10.2	56.2	126.8	140.9	266.9
EC-g-PHBV$_{1.8}$	0.71	39.1	49.0	36.6	51.8	113.1	136.5	266.3
EC-g-PHBV$_{2.1}$	0.74	39.9	65.7	36.2	62.2	124.1	139.1/145.3	271.3

[a] The ratio for the copolymers was calculated from the FT-IR spectra.
[b] X_c was calculated from the WAXD patterns.

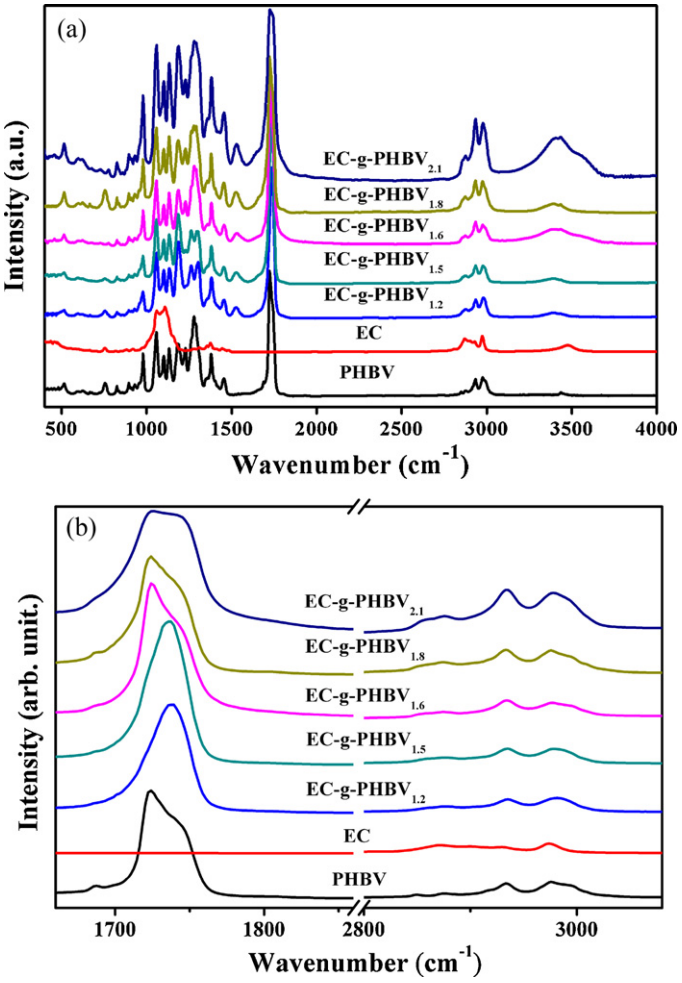

Fig. 2. FT-IR spectra of PHBV, EC and the resulting copolymers prepared under various HDI/PHBV fractions. (a) Total spectra and (b) carbonyl and alkyl bands.

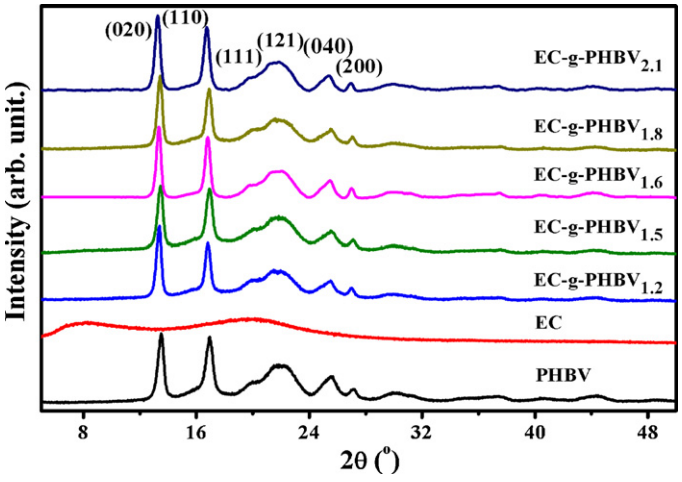

Fig. 3. WAXD patterns of PHBV, EC and the resulting copolymers prepared under various HDI/PHBV fractions.

than relatively short one (Zhu et al., 2010). However, the strong spacial restriction of relatively long side-chains, and even entanglement between long side-chains with high grafting density are usually appeared in the copolymers, thus the mobility of crystalline PHBV chain would be restricted. The easier the mobility of the side chains, the larger the amorphous regions of the copolymers. Therefore, with an increase of the lengths and grafting density of PHBV side chain, the equilibrium between the mobility and restriction of crystalline PHBV chain would greatly influence the degree of crystallinity of the copolymers. For those copolymers with more long PHBV side chains, such as EC-g-PHBV$_{2.1}$ have more crystalline domains, whereas the copolymers (EC-g-PHBV$_{1.8}$) with relatively board length distribution and more short side chains contributed to larger amorphous domains.

3.3. Crystal structure: WAXD

Fig. 3 shows the WAXD patterns of PHBV, EC and the resulting copolymers. Two broad peaks at 7.5° and 20.8° in the patterns of EC implied the amorphous structure of EC (Zhu et al., 2010). The

peaks at 13.3°, 16.8°, 21.4°, 25.6°, 27.2° and 29.9° were assigned to (0 2 0), (1 1 0), (1 1 1), (1 2 1), (0 4 0) and (2 0 0) planes of PHBV, respectively, and the unit cells of 3HB and 3HV in PHBV belonged to the orthorhombic crystal system (Bluhm & Hamer, 1986; Sato et al., 2004). These similar peaks appeared in the diffraction patterns of the copolymers, and only slight decrease in the peak intensities can be observed. This indicated that the movements of the PHBV side chains were hindered due to the spacial restrictions, inducing the decrease in the crystallization ability. These changes were in accordance with the results from FT-IR spectra. Further, a transition in the intensity for the (2 0 0) plane can be observed. It is found that the intensities gradually increased with the increasing of the HDI/PHBV fraction from 1.2 to 1.6, then decreased for 1.8, and finally increased for 2.1. It has been demonstrated that the increase in the intensity of (2 0 0) peak could be contributed to the preferential growth of PHBV crystals along the direction of the α axis (Bluhm & Hamer, 1986). Therefore, the crystal growth of PHBV along the direction of α axis was restricted to some extent in the copolymers.

Table 2 listed the degree of crystallinity (X_c) of PHBV and the copolymers. It is clear that X_c of the copolymers were lower than 58.1% for neat PHBV. EC as an amorphous polymer can suppress and break the crystalline domains of crystalline polymers (Yan et al., 2009; Yuan et al., 2007; Zhu et al., 2010), thus the crystallization of PHBV in copolymers would be restricted, resulting in the imperfection of PHBV crystal. With the increase of the HDI/PHBV fraction, the X_c of the copolymers decreased gradually from 43.6% for EC-g-PHBV$_{1.2}$ to 39.1% for EC-g-PHBV$_{1.8}$, and then increased to 39.9% for EC-g-PHBV$_{2.1}$. The decrease in X_c implied that relatively board length distribution and high grafting density of PHBV side chain appeared in the copolymer, which induced the crystal imperfection mainly due to the short chain length of PHBV segments in copolymers. However, for EC-g-PHBV$_{2.1}$, more long side chain with high grafting density of PHBV segments would give more fluidity and be easily prone to crystallize. Therefore, a significant transition in the X_c can be observed. The similar phenomenon has been observed through grafting various lengths of PPDO side chains on EC backbone (Zhu et al., 2010).

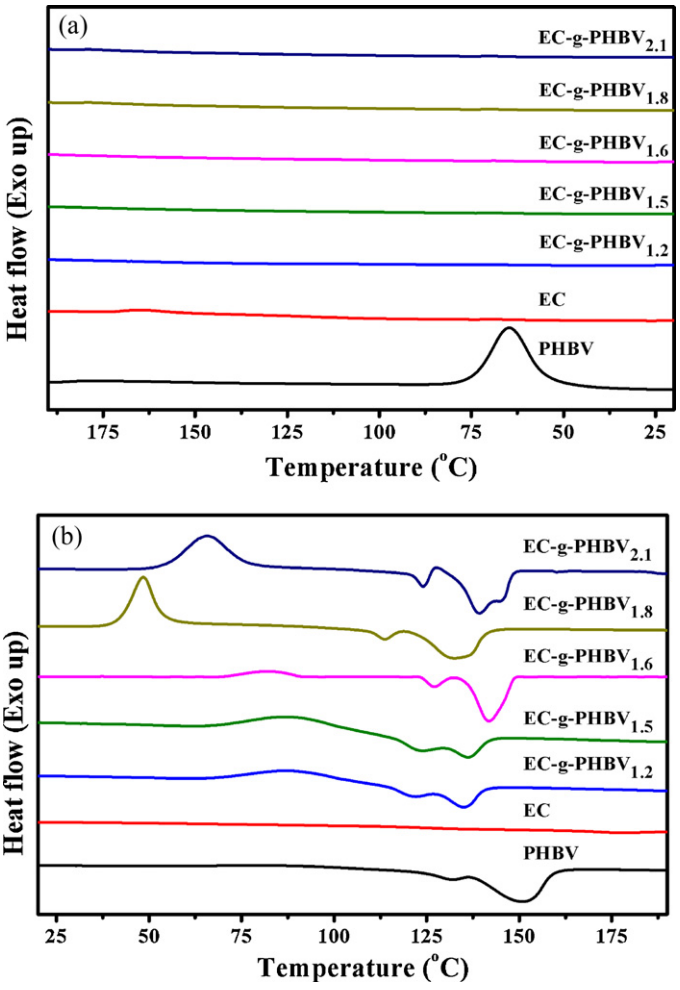

Fig. 4. DSC traces of PHBV, EC and the resulting copolymers prepared under various HDI/PHBV fractions obtained during the first cooling (a) and second heating (b) scans at a rate of 10 °C min^{-1}.

3.4. Crystallization behavior: DSC

The degradation of polyesters began in the amorphous zone and then the crystalline zone. The degree of crystallinity plays a significant role in the physical properties and biodegradability of biodegradable polymers. Fig. 4 shows the DSC curves of PHBV, EC and the resulting copolymers during first cooling (a) and second heating processes (b), and the corresponding thermal parameters are listed in Table 2. In general, the second heating run was used to measure the crystal structure formed during the non-isothermal crystallization. It is observed that a broad and strong crystallization peak for neat PHBV disappeared in copolymers during the first cooling trace, and the double melting peaks remained during the second heating run. The double melting peak located at 135.9 and 150.9 °C for neat PHBV can be formed through a melting, recrystallization and remelting process (Liu et al., 2009). Compared with that of neat PHBV, all the copolymers prepared at the different HDI/PHBV fractions exhibited similar double melting peaks, but their peak positions have great difference. Therefore, it can be indicatory that the crystallization ability of copolymers was greatly influenced by their grafting structures. Generally, the melting point from the relatively high temperature endotherm such as the second melting point (T_{m2}), was usually taken as the true melting temperature for the copolymers (Liu et al., 2009). The data presented in Table 2 indicate that the T_{m2} values of all the copolymers were lower than that of neat PHBV (150.9 °C). With the HDI/PHBV fraction varied from 1.2 to 1.6, T_{m2} of the copolymers shifted from 134.8 to 140.9 °C, and the heat of fusion (ΔH_m) increased from 10.1 to 56.2 J g^{-1}. As far as we know, the higher the DP and DS of the graft polymers, the higher the melting temperature and the heat of fusion (Zhu et al., 2010). Once the HDI/PHBV fraction reached to 1.8, the T_{m2} decreased to 136.5 °C with ΔH_m of 51.8 J g^{-1}. This further supported that EC-g-PHBV$_{1.8}$ had the more boarder side-chain length distribution than other copolymers, which was consistent with the NMR results. For EC-g-PHBV$_{2.1}$, T_{m2} shifted to higher temperature with the ΔH_m of 62.2 J g^{-1}, and the corresponding melting peak included a main melting peak at 139.1 °C with a new shoulder at 145.3 °C. This indicated an improvement in the crystal perfection of copolymers, just like in grafting PCL and PPDO into cellulosic materials (Yan et al., 2009; Yuan et al., 2007; Zhu et al., 2010). From above, both T_m and X_c can be adjusted by simply modulating the HDI/PHBV fraction to meet the requirements of medical applications of the resulting copolymers.

No obvious peak for neat PHBV appeared in the cold crystallization process. However, a weak and board cold crystallization peak could be observed for the copolymers, and the change in the crystallization behavior showed a significant transition exhibition as shown in Fig. 4(b). With the increasing of the HDI/PHBV fraction, the cold crystallization peak became gradually more strong, and the cold crystallization temperature (T_{cc}) decreased from 86.8 °C for EC-g-PHBV$_{1.2}$ to 49.0 °C for EC-g-PHBV$_{1.8}$, and then increased to 65.7 °C for EC-g-PHBV$_{2.1}$. Accordingly, the cold crystallization enthalpy (ΔH_{cc}) increased from 4.3 to 36.6 J g^{-1}, and then decreased to 36.2 J g^{-1}. For relatively low HDI/PHBV fraction,

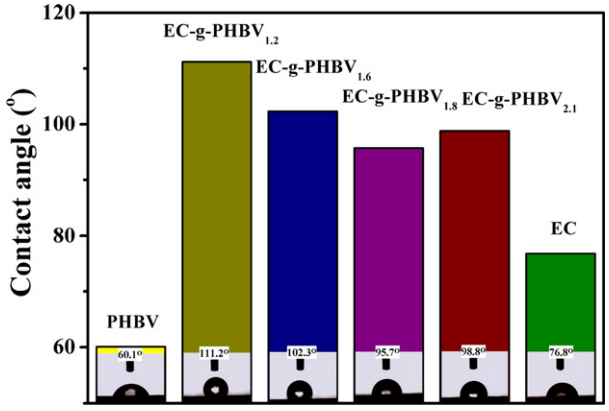

Fig. 5. The contact angles of PHBV, EC and the resulting copolymers prepared under various HDI/PHBV fractions.

the copolymers with relatively short side chains and low grafting density possessed the strong crystallization ability, but more crystal defects. When the grafting density of PHBV side chains was high enough, the cold crystallization of the copolymers would be enhanced. For EC-g-PHBV$_{2.1}$, the spacial restriction effect and especially entanglement between long PHBV side chains became obvious, which resulted in relative difficulty for the cold crystallization of the copolymer, thus the cold crystallization peak became more board and shifted to higher temperature. The similar influence of the grafting density on the cold crystallization has been observed in grafting poly(ε-caprolactone) or PPDO side chains on EC backbone (Yan et al., 2009; Yuan et al., 2007; Zhu et al., 2010).

3.5. Thermal stability: TGA

The effects of the length and grafting density of PHBV side chains on the thermal stability of the copolymers were studied under N_2 atmosphere, and the corresponding thermal parameters were listed in Table 2. Thermal degradation through a one-step process can be observed, and the thermal stability of the copolymers was better than that for neat PHBV at 259.6 °C, but poorer than that for EC at 364.4 °C. This result can be ascribed to the covalent bond between PHBV chains and EC backbone, less thermally unstable hydroxyl groups in the copolymer and the residual hydrogen bonds in the original structure of EC after grafting PHBV chains. It has been reported that less the hydroxyl groups of side chains, the better the thermal stability of the copolymers (Yuan et al., 2007). Furthermore, as shown in Table 2, T_{max} exhibited similar trend as well as X_c. With the increasing of the HDI/PHBV fraction, T_{max} decreased from 272.6 °C for EC-g-PHBV$_{1.2}$ to 266.3 °C for EC-g-PHBV$_{1.8}$, and then increased to 271.4 °C for EC-g-PHBV$_{2.1}$. The decrease in the T_{max} can be attributed to two factors. One of them is the crystal imperfection, which was mainly caused by the board length distribution and a number of short PHBV side chains in copolymers. Another factor would be the thermally unstable hydroxyl groups of the materials, more hydroxyl groups from short PHBV chains could depress the thermal stability of the polymer, such as EC-g-PHBV$_{1.8}$. Therefore, once more long side chains and high grafting density presented in the copolymer, such as EC-g-PHBV$_{2.1}$, its thermal stability can be improved significantly.

3.6. Hydrophobic property: contact angle measurement

Fig. 5 gave the contact angles of PHBV, EC and the resulting copolymer films determined by deionized water via the static contact angle measurement. It is found that the copolymers generally have larger contact angle than 60.1° for neat PHBV and 76.8° for EC. With the increasing of the HDI/PHBV fractions, the contact angle of the copolymer gradually decreased from 111.2° for EC-g-PHBV$_{1.2}$ to 95.7° EC-g-PHBV$_{1.8}$, and then increased to 98.8° for EC-g-PHBV$_{2.1}$. For EC-g-PHBV$_{1.8}$ with more hydroxyl groups of short chains exhibited more hydrophilic than other copolymers. Among these copolymers, the EC-g-PHBV$_{1.2}$ showed the most hydrophobic with contact angle of 111.2°, which was close to that for well-studied block poly(ester-urethane) poly(3/4HB-HHxHO) urethanes (water contact angle 88–117°) as a strong platelet adhesion for blood coagulation (Chen, Cheng, Xu, et al., 2009). It is well known that the hydrophilicity/hydrophobicity balance is an important factor to affect the platelet adhesion and the biocompatibility of materials, the strong platelet adhesion property and good biocompatibility would endow the copolymers as a potential candidate for wound healing applications as hemostatic materials (Chen, Cheng, Li, et al., 2009; Chen, Cheng, Xu, et al., 2009). In addition, the lowered crystallinity in copolymers was beneficial to the penetration of water molecule into amorphous regions, which would result in a distinct acceleration of the cleavage of PHBV side-chains.

4. Conclusions

A series of biodegradable EC-g-PHBV copolymers were prepared through the homogeneous acylation reaction between EC and telechelic OH-terminated PHBV as an oligomer at a constant mass ratio of PHBV to EC of 4:1, in which HDI was used as coupling agent and dibutyltin dilaurate as catalyst in 1,2-dichloroethane. The crystallinity and hydrophobicity of the copolymers could be modulated through changing the HDI/PHBV fraction to control the length and grafting density of PHBV side chains. It is found that a transition exhibition occurred on the crystallization and thermal degradation behavior of the copolymers. With the increasing of the HDI/PHBV fraction, the degree of crystallinity decreased from 58.1% for neat PHBV to 39.1% for EC-g-PHBV$_{1.8}$, and then increased again to 39.9% for EC-g-PHBV$_{2.1}$, while T_{max} increased from 259.6 °C for neat PHBV to 271.4 °C for EC-g-PHBV$_{2.1}$. Moreover, the copolymers became more hydrophobic (water contact angle 95.7–111.2°) than the neat PHBV materials. Most importantly, an efficient approach is presented to obtain the expected graft copolymers with the modulated crystallinity, better thermal stability, and favorable biocompatibility and so on, and these copolymers exhibited great potential for their applications as desired scaffolds for tissue engineering and hemostatic materials.

Acknowledgements

This work was supported by the key basic research foundation of the Committee of Science and Technology of Shanghai Municipality (Grant no. 06JC14003), and the Fundamental Research Funds for the Central Universities as well as the Doctorate Innovation Foundation of Donghua University (BC201101).

References

Aggour, Y. A., & Abdel-Razik, E. A. (1999). Graft copolymerization of end allenoxy polyoxyethylene macromonomer onto ethyl cellulose in a homogeneous system. *European Polymer Journal*, *35*, 2225–2228.

Bhardwaj, R., Mohanty, A. K., Drzal, L. T., Pourboghrat, F., & Misra, M. (2006). Renewable resource-based green composites from recycled cellulose fiber and poly(3-hydroxybutyrate-co-3-hydroxyvalerate) bioplastic. *Biomacromolecules*, *7*, 2044–2051.

Bluhm, T. L., & Hamer, G. K. (1986). Studies of composition and crystallinity of bacterial poly(β-hydroxybutyrate-co-β-hydroxyvalerate). *Macromolecules*, *19*, 2865–2871.

Ceccorulli, G., Pizzoli, M., & Scandola, M. (1993). Effect of a low molecular weight plasticizer on the thermal and viscoelastic properties of miscible blends of bacterial poly(3-hydroxybutyrate) with cellulose acetate butyrate. *Macromolecules*, *26*, 6722–6726.

Chen, G. Q., & Wu, Q. (2005). The application of polyhydroxyalkanoates as tissue engineering materials. *Biomaterials*, *26*, 6565–6578.

Chen, Z., Cheng, S., Li, Z., Xu, K., & Chen, G. Q. (2009). Synthesis, characterization and cell compatibility of novel poly(ester urethane)s based on poly(3-hydroxybutyrate-co-4-hydroxybutyrate) and poly(3-hydroxybutyrate-co-3-hydroxyhexanoate) prepared by melting polymerization. *Journal of Biomaterials Science*, *20*, 1451–1471.

Chen, Z., Cheng, S., & Xu, K. (2009). Block poly(ester-urethane)s based on poly(3-hydroxybutyrate-co-4-hydroxybutyrate) and poly(3-hydroxyhexanoate-co-3-hydroxyoctanoate). *Biomaterials*, *30*, 2219–2230.

Finelli, L., Scandola, M., & Sadocco, P. (1998). Biodegradation of blends of bacterial poly(3-hydroxybutyrate) with ethyl cellulose in activated sludge and in enzymatic solution. *Macromolecular Chemistry and Physics*, *199*, 695–703.

Ha, C. S., & Cho, W. J. (2002). Miscibility, properties, and biodegradability of microbial polyester containing blends. *Progress in Polymer Science*, *27*, 759–809.

Hirt, T. D., Neuenschwander, P., & Suter, U. W. (1996). Telechelic diols from poly[(R)-3-hydroxybutyric acid] and poly{[(R)-3-hydroxybutyric acid]-co-[(R)-3-hydroxyvaleric acid]}. *Macromolecular Chemistry and Physics*, *197*, 1609–1614.

Hu, S. G., Jou, C. H., & Yang, M. C. (2004). Biocompatibility and antibacterial activity of chitosan and collagen immobilized poly(3-hydroxybutyric acid-co-3-hydroxyvaleric acid). *Carbohydrate Polymers*, *58*, 173–179.

Hu, Y. J., Wei, X., Zhao, W., Liu, Y. S., & Chen, G. Q. (2009). Biocompatibility of poly(3-hydroxybutyrate-co-3-hydroxyvalerate-co-3-hydroxyhexanoate) with bone marrow mesenchymal stem cells. *Acta Biomaterialia*, *5*, 1115–1125.

Jack, K. S., Velayudhan, S., Luckman, P., Trau, M., Grodahl, L., & Cooper-White, J. (2009). The fabrication and characterization of biodegradable HA/PHBV nanoparticle-polymer composite scaffolds. *Acta Biomaterialia*, *5*, 2657–2667.

Jansen, E. J. P., Sladek, R. E. J., Bahar, H., Yaffe, A., Gijbels, M. J., Kuijer, R., et al. (2005). Hydrophobicity as a design criterion for polymer scaffolds in bone tissue engineering. *Biomaterials*, *26*, 4423–4431.

Ke, Y., Wang, Y. J., Renb, L., Zhao, Q. C., & Huang, W. (2010). Modified PHBV scaffolds by in situ UV polymerization: Structural characteristic, mechanical properties and bone mesenchymal stem cell compatibility. *Acta Biomaterialia*, *6*, 1329–1336.

Langer, R., & Tirrell, D. A. (2004). Designing materials for biology and medicine. *Nature*, *428*, 487–492.

Lao, H. K., Renard, E., Linossier, I., Langlois, V., & Vallée-Rehel, K. (2007). Modification of poly(3-hydroxybutyrate-co-3-hydroxyvalerate) film by chemical graft copolymerization. *Biomacromolecules*, *8*, 416–423.

Li, X., Liu, K. L., Wang, M., Wong, S. Y., Tjiu, W. C., He, C. B., et al. (2009). Improving hydrophilicity, mechanical properties and biocompatibility of poly[(R)-3-hydroxybutyrate-co-(R)-3-hydroxyvalerate] through blending with poly[(R)-3-hydroxybutyrate]-alt-poly(ethylene oxide). *Acta Biomaterialia*, *5*, 2002–2012.

Liu, Q. S., Zhu, M. F., Wu, W. H., & Qin, Z. Y. (2009). Reducing the formation of six-membered ring ester during thermal degradation of biodegradable PHBV to enhance its thermal stability. *Polymer Degradation and Stability*, *94*, 18–24.

Kang, H., Liu, W., He, B., Shen, D., Ma, L., & Huang, Y. (2006). Synthesis of amphiphilic ethyl cellulose grafting poly(acrylic acid) copolymers and their self-assembly morphologies in water. *Polymer*, *47*, 7927–7934.

Kose, G. T., Tezcaner, A., & Hasirci, V. (2002). Fundamentals of tissue engineering: Carrier materials and an application. *Technology and Health Care*, *10*, 187–201.

Sato, H., Nakamura, M., Padermshoke, A., Yamaguchi, H., Terauchi, H., Ekgasit, S., et al. (2004). Thermal behavior and molecular interaction of poly(3-hydroxybutyrateco-3-hydroxyhexanoate) studied by wide-angle X-ray diffraction. *Macromolecules*, *37*, 3763–3769.

Sultana, N., & Wang, M. (2008). PHBV/PLLA-based composite scaffolds containing nano-sized hydroxyapatite particles for bone tissue engineering. *Journal of Experimental Nanoscience*, *3*, 121–132.

Suthar, V., Pratap, A., & Raval, H. (2000). Studies on poly (hydroxyl alkanoates)/(ethylcellulose) blends. *Bulletin of Materials Science*, *23*, 215–219.

Yan, Q., Yuan, J., Zhang, F., Sui, X., Xie, X., Yin, Y., et al. (2009). Cellulose-based dual graft molecular brushes as potential drug nanocarriers: Stimulus-responsive micelles, self-assembled phase transition behavior, and tunable crystalline morphologies. *Biomacromolecules*, *10*, 2033–2042.

Yoshie, N., Saito, M., & Inoue, Y. (2004). Effect of chemical compositional distribution on solid-state structure and properties of poly(3-hydroxybutyrate-co-3-hydroxyvalerate). *Polymer*, *45*, 1903–1911.

Yu, L., Dean, K., & Li, L. (2006). Polymer blends and composites from renewable resources. *Progress in Polymer Science*, *31*, 576–602.

Yuan, W., Yuan, J., Zhang, F., & Xie, X. (2007). Syntheses, characterization, and in vitro degradation of ethyl cellulose-graft-poly(ε-caprolactone)-block-poly(L-lactide) copolymers by sequential ring-opening polymerization. *Biomacromolecules*, *8*, 1101–1108.

Zhang, L., Deng, X., & Huang, Z. (1997). Miscibility, thermal behavior and morphological structure of poly(3-hydroxybutyrate) and ethyl cellulose binary blends. *Polymer*, *38*, 5379–5387.

Zhu, J., Dong, X. T., Wang, X. L., & Wang, Y. Z. (2010). Preparation and properties of a novel biodegradable ethyl cellulose grafting copolymer with poly(p-dioxanone) side-chains. *Carbohydrate Polymers*, *80*, 350–359.